


Enhancement of Long-Persistent Phosphorescence by Solid-State Reaction and Mixing of Spectrally Different Phosphors

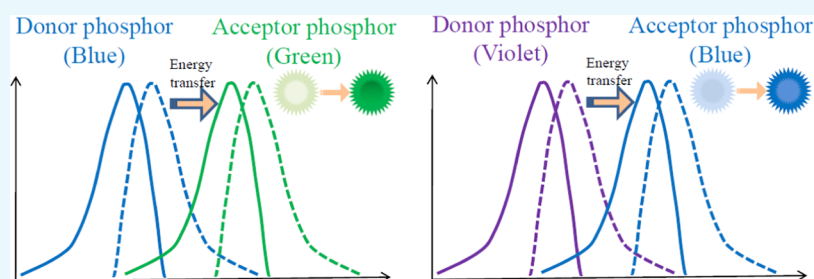
Doory Kim,* Han-Eol Kim, and Chang-Hong Kim

Cite This: *ACS Omega* 2020, 5, 10909–10918

Read Online

ACCESS |

 Metrics & More

 Article Recommendations


ABSTRACT: Rare-earth-doped oxide-based phosphors have attracted great interest as light-emitting materials for technical applications and fundamental research because of their high brightness, tunable emission wavelength, and low toxicity, as well as chemical and thermal stability. The recent development of rare-earth-doped nanostructured materials showed improved phosphorescence characteristics, including afterglow and lifetime. However, the development of highly efficient phosphors remains challenging in terms of brightness and long persistence. Herein, novel protocols were developed for improving phosphorescence characteristics based on the energy transfer effect by chemical mixing of spectrally different phosphors. This protocol is based on the simple mixing method of different phosphors, which is totally different from the conventional methods but provides much brighter persistent phosphorescence. Simple chemical mixing methods significantly improved the afterglow intensity and lifetime of green and blue phosphors regardless of mixed time when subjected to a high-temperature solid-state reaction. In particular, chemical mixing after a high-temperature solid-state reaction enhanced the phosphorescence intensity more effectively than did chemical mixing before the reaction. We achieved increased luminescence of the phosphor, which is 10 times greater than that of the control sample, from all of the chemical mixing methods, which resulted in more efficient energy transfer than previously reported studies. Chemical mixing of three spectrally different phosphors was also performed to achieve multistep energy transfer for the first time, exhibiting a much higher afterglow intensity (~ 2 times) than that of single-step energy transfer. This study provides a novel and simple method for the production of bright and long-persistent phosphors and thus expands their application range.

INTRODUCTION

Phosphor materials have attracted considerable interest for fundamental research and technical applications due to their wide range of applications in organic light-emitting devices (OLEDs), for energy saving, and for safety improvement. Because of these wide-ranging applications, improving the brightness and increasing the decay time of the phosphor are challenging. While sulfide-based phosphors suffer from rapid degradation, rare-earth-doped oxide-based phosphors are chemically and thermally stable.¹ The high heat resistance, high brightness, long persistence time, low toxicity, and tunable emission wavelength from the UV to visible range make them suitable phosphor materials.^{2–8} It leads to wide applications, such as usage in solid-state lasers, fluorescent lamps, cathode ray tubes, field emission display (FED) devices, plasma display panels (PDP), fiber amplifiers, radiation dosimetry, optoelectronics for image storage, X-ray imaging, noncontact temperature sensing, etc.^{9,10}

Therefore, substantial efforts toward the improvement of phosphorescence characteristics by systematic investigations into the preparation, composition, structure, and luminescence properties of rare-earth-doped nanostructured materials have been made.^{11–14} For example, Kim et al. developed novel green- (SrAl₂O₄:Eu²⁺, Dy³⁺) and blue-emitting phosphors (CaAl₂O₄:Eu²⁺), which exhibited extremely bright and long-lasting phosphorescence.^{11,12} By comparing various compositions of the activator (Eu²⁺) and coactivator (Dy³⁺), as well as impurities, the optimal conditions were determined. In a similar manner, Yu et al. reported that the luminescence

Received: February 11, 2020

Accepted: April 24, 2020

Published: May 5, 2020



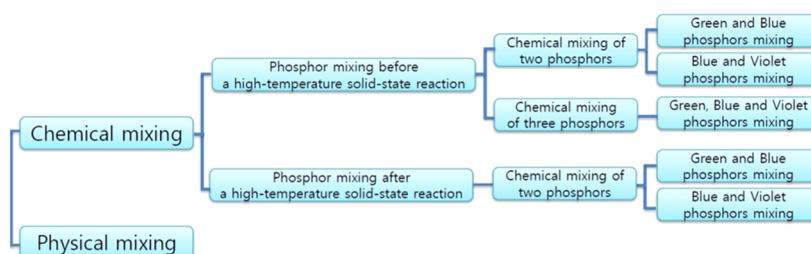


Figure 1. Different phosphor mixing methods used in this study.

efficiency of $\text{SrZnO}_2:\text{Eu}^{3+}$ can be improved by co-doping with alkali metal ions such as Li^+ , Na^+ , and K^+ .^{13,13} The photoluminescence intensity of the red-light-emitting cubic $\text{Zr}_{0.99}\text{Eu}_{0.01}\text{O}_2$ was enhanced by doping with lithium.¹⁴ Tb^{3+} -doped calcium and strontium aluminates (CaAl_2O_4 , $\text{CaAl}_2\text{O}_4:\text{Tb}^{3+}$, SrAl_2O_4 , $\text{SrAl}_2\text{O}_4:\text{Tb}^{3+}$) were also synthesized, and the effect of the preparation method on the photoluminescence properties was investigated.¹⁵ The afterglow brightness of Eu^{2+} -doped BaAl_2O_4 was also enhanced by doping with a second rare-earth activator including La, Ce, Pr, Nd, Sm, Gd, Tb, Dy, Er, and Tm.¹⁶

Although recent studies have improved the phosphorescence quantum yield of phosphors, it remains highly desirable to develop more efficient phosphors for existing and novel applications. Herein, the effects of energy transfer between different colored phosphors were investigated, focusing on the phosphorescence of green- and blue-emitting alkaline-earth aluminate phosphors ($\text{SrAl}_2\text{O}_4:\text{Eu}^{2+}$, Dy^{3+} and $\text{Sr}_4\text{Al}_{14}\text{O}_{25}:\text{Eu}^{3+}$, Dy^{3+}) to improve their phosphorescence characteristics. The energy transfer between two light-sensitive molecules has been applied for measuring the separation distance and probing molecular interactions between fluorophores, known as the Förster resonance energy transfer (FRET).¹⁷ The energy from an excited donor chromophore is transferred to another acceptor chromophore via nonradiative dipole–dipole coupling. The theoretical rate of the FRET depends on the extent of spectral overlap between the donor emission and acceptor absorption spectra. Recently, several groups have reported the energy transfer from donor ions to acceptor ions in phosphors. For example, Caldino et al. reported the energy transfer effect in $\text{CaCl}_2:\text{Eu}^{2+}$, Mn^{2+} single crystals.¹⁸ Barry et al. and Yao et al. investigated $\text{Eu}^{2+} \rightarrow \text{Mn}^{2+}$ energy transfer in $\text{BaMg}_2\text{Si}_2\text{O}_7$, whereas Yang et al. reported a similar effect in the Eu^{2+} - and Mn^{2+} -coactivated $\text{CaAl}_2\text{Si}_2\text{O}_8$ phosphors, all of which involved $\text{Eu}^{2+} \rightarrow \text{Mn}^{2+}$ energy transfer in the same host crystal.^{19–21} The electron transfer in $\text{Er}^{3+}/\text{Yb}^{3+}$ -co-doped phosphors has been reported as well. Several groups have reported that the energy is transferred from Yb^{3+} (donor) to Er^{3+} (acceptor), resulting in the upconversion luminescence process in various host materials.¹⁰ The energy transfer from Bi^{3+} to Eu^{3+} was also observed in $\text{Ba}_2\text{Y}(\text{BO}_3)_2\text{Cl}:\text{Bi}^{3+}$, Eu^{3+} phosphors. It has been suggested that the spectral overlapping between the emission bands of Bi^{3+} and the excitation peaks of Eu^{3+} supports the energy transfer from Bi^{3+} to Eu^{3+} by an electric dipole–dipole interaction.²² The energy transfer phenomenon from Ce^{3+} to Tb^{3+} has also been demonstrated for various Ce^{3+} , Tb^{3+} co-doped phosphors ($\text{BaLu}_6(\text{Si}_2\text{O}_7)_2(\text{Si}_3\text{O}_{10}):\text{Ce}^{3+}, \text{Tb}^{3+}$) by observing the change in emission spectra and decay lifetimes with different doped concentrations.^{23–25} This mechanism has been proved to be an electric dipole–dipole interaction.^{23,24} As documented in the literature, it is generally agreed that the energy transfer can take place in various phosphate phosphors,

and an electric dipole–dipole interaction has been suggested to support their mechanism. However, to the best of our knowledge, all of the studies on energy transfer in phosphors are primarily focused on the energy transfer in single host materials and no investigations regarding energy transfer between different host crystals have been reported to date.

In this study, a novel and simple synthesis technique was developed by applying the energy transfer between spectrally similar phosphors with different host crystals to increase the phosphorescence quantum yield of phosphors. This is a completely different approach from conventional processes such as solid-state reactions with various compositions and electron transfer mechanism-based doping methods in single host crystals. Since this novel method can be extended to a number of combinations of donor and acceptor, it can thus offer greater variation in the energy transfer processes than the conventional energy transfer process-based methods. Conventional methods are limited to the energy transfer between the co-dopants in single host materials. Moreover, we have demonstrated the multistep energy transfer in phosphors for the first time, which exhibits much higher afterglow intensity than conventional single-step energy transfer. This study is, therefore, expected to provide a novel and simple method for the production of bright and long-persistent phosphors and thus expand their application range.

RESULTS

Herein, several synthetic methods are presented by mixing spectrally different phosphors to examine the energy transfer effect in detail. Because the energy transfer efficiency depends on the extent of spectral overlap between the donor emission and acceptor absorption spectra, a higher phosphorescence efficiency is expected from the spectrally close donor phosphors.¹⁷ For example, energy from the blue-emitting calcium aluminate phosphor should be transferred to the green-emitting alkaline-earth aluminate phosphor ($\text{SrAl}_2\text{O}_4:\text{Eu}^{2+}$, Dy^{3+}), improving the phosphorescence efficiency of the green-emitting phosphor. In the same manner, the phosphorescence efficiency of the blue-emitting phosphor should be improved by the energy transfer from a violet-emitting to blue-emitting phosphor. To obtain a large spectral overlap between the phosphor pairs to achieve a high energy transfer rate, alkaline-earth aluminate phosphors ($\text{SrAl}_2\text{O}_4:\text{Eu}^{2+}$, Dy^{3+} and $\text{Sr}_4\text{Al}_{14}\text{O}_{25}:\text{Eu}^{2+}$, Dy^{3+}) and calcium aluminate phosphor ($\text{CaAl}_2\text{O}_4:\text{Eu}^{2+}$, Nd^{3+}) were chosen as green-, blue-, and violet-emitting phosphors, respectively.^{1,13}

Two different approaches can be used to mix spectrally different phosphors, chemical or physical mixing (Figure 1). In physical mixing, the spectrally different phosphors are first synthesized via a high-temperature solid-state reaction, and then they are mixed at room temperature. In contrast, in

chemical mixing, different phosphors are mixed at a high temperature. We tried two chemical mixing approaches: (1) all starting materials for different phosphors were first mixed and subjected to a high-temperature solid-state reaction and (2) the separately synthesized different phosphors via high-temperature solid-state reactions are mixed and then fired at high temperatures. The distance between the spectrally different phosphors mixed using the chemical mixing approach is expected to be shorter than that obtained using physical mixing, allowing for more effective energy transfer between the spectrally different phosphors. Therefore, the chemical mixing approach was used to enhance the phosphorescence intensity herein. In the chemical mixing method, two different approaches can be used depending on whether different phosphors are mixed before or after a high-temperature solid-state reaction, as shown in Figure 1. (1) The starting materials of different phosphors are mixed in a particular ratio before the high-temperature solid-state reaction, and the mixture is subsequently fired in horizontal tube furnaces. (2) Spectrally different phosphors are synthesized separately via a high-temperature solid-state reaction, and the mixture is subsequently fired with H_3BO_3 at 800–1400 °C after the synthesized samples are mixed in a certain ratio using an agate mortar. In the first approach, the distance between the spectrally different phosphors in the sample can be very short (to the atomic scale). In the second approach, the distance between the spectrally different phosphors is expected to be of a phosphor particle size level. Herein, these two chemical mixing approaches using different ratios of green-, blue-, and violet-emitting phosphors were examined to maximize the energy transfer efficiency.

Chemical Mixing of Two Phosphors via High-Temperature Solid-State Reaction. Using this approach, the starting materials of green ($\text{SrAl}_2\text{O}_4:\text{Eu}^{2+}, \text{Dy}^{3+}$) and blue ($\text{Sr}_4\text{Al}_{14}\text{O}_{25}:\text{Eu}^{3+}, \text{Dy}^{3+}$) phosphors were first mixed in a particular ratio, as shown in Table 1, to enhance the phosphorescence of the green phosphor ($\text{SrAl}_2\text{O}_4:\text{Eu}^{2+}, \text{Dy}^{3+}$). Next, the mixed powders were fired in horizontal tube furnaces for the high-temperature solid-state reaction. To investigate the energy transfer effect depending on the ratio between two phosphors, the afterglow of the samples prepared with green phosphor:blue phosphor (G:B) molar ratios ranging from 10:0 to 5:5 was examined. The green phosphor ($\text{SrAl}_2\text{O}_4:\text{Eu}^{2+}$) exhibited a broad-band emission spectrum peaking at 520 nm, as shown in Figure 2, which can be attributed to the $4f \rightarrow 5d$ transition of Eu^{2+} .¹³ Thus, the afterglow intensity was monitored at the emission peak of ~520 nm at room temperature to measure the energy transfer effect from the blue phosphor on the phosphorescence intensity of the green phosphor. Figure 3A,B shows the decay curves for phosphors synthesized with different ratios of green and blue phosphors. The initial afterglow intensity measured at 5 s changed significantly as a function of the G:B molar ratio, as shown in Figure 3C. Increased luminescence (>10 times) relative to the control sample (green phosphor only) was observed at a G:B ratio of 5:5. The lifetimes were calculated by fitting the decay curves with three exponential components, and these photophysical results are listed in Table 2 and Figure 3D. The decay time of luminescence of the green phosphor was increased as the relative amount of blue phosphor increased, indicating the effective energy transfer from the blue to green phosphor, as expected. Therefore, the energy transfer between the spectrally different phosphors is

Table 1. Procedure and Reagents in Each Step for Different Mixing Methods

phosphor mixing before a high-temperature solid-state reaction	procedure	Step 1				Step 2		Step 3		Step 4		
		reagents for phosphor 1		reagents for phosphor 2		reagents for phosphor 3		reagents for phosphor 4		reagents for phosphor 5		
green and blue phosphors mixing	green and blue phosphors mixing	phosphor 1 ($\text{SrAl}_2\text{O}_4:\text{Eu}^{2+}, \text{Dy}^{3+}$)	phosphor 2 ($\text{Sr}_4\text{Al}_{14}\text{O}_{25}:\text{Eu}^{3+}, \text{Dy}^{3+}$)	phosphor 3 ($\text{SrCO}_3, \text{CaCO}_3, \text{Al}_2\text{O}_3, \text{Eu}_2\text{O}_3, \text{Dy}_2\text{O}_3, \text{H}_3\text{BO}_3, \text{SiO}_2, \text{Li}_2\text{CO}_3$)	phosphor 4 ($\text{SrCO}_3, \text{CaCO}_3, \text{Al}_2\text{O}_3, \text{Eu}_2\text{O}_3, \text{Dy}_2\text{O}_3, \text{H}_3\text{BO}_3, \text{SiO}_2, \text{Li}_2\text{CO}_3$)	phosphor 5 ($\text{SrCO}_3, \text{CaCO}_3, \text{Al}_2\text{O}_3, \text{Eu}_2\text{O}_3, \text{Dy}_2\text{O}_3, \text{H}_3\text{BO}_3, \text{SiO}_2, \text{Li}_2\text{CO}_3$)	phosphor 6 ($\text{SrCO}_3, \text{CaCO}_3, \text{Al}_2\text{O}_3, \text{Eu}_2\text{O}_3, \text{Dy}_2\text{O}_3, \text{H}_3\text{BO}_3, \text{SiO}_2, \text{Li}_2\text{CO}_3$)	phosphor 7 ($\text{SrCO}_3, \text{CaCO}_3, \text{Al}_2\text{O}_3, \text{Eu}_2\text{O}_3, \text{Dy}_2\text{O}_3, \text{H}_3\text{BO}_3, \text{SiO}_2, \text{Li}_2\text{CO}_3$)	phosphor 8 ($\text{SrCO}_3, \text{CaCO}_3, \text{Al}_2\text{O}_3, \text{Eu}_2\text{O}_3, \text{Dy}_2\text{O}_3, \text{H}_3\text{BO}_3, \text{SiO}_2, \text{Li}_2\text{CO}_3$)	phosphor 9 ($\text{SrCO}_3, \text{CaCO}_3, \text{Al}_2\text{O}_3, \text{Eu}_2\text{O}_3, \text{Dy}_2\text{O}_3, \text{H}_3\text{BO}_3, \text{SiO}_2, \text{Li}_2\text{CO}_3$)	phosphor 10 ($\text{SrCO}_3, \text{CaCO}_3, \text{Al}_2\text{O}_3, \text{Eu}_2\text{O}_3, \text{Dy}_2\text{O}_3, \text{H}_3\text{BO}_3, \text{SiO}_2, \text{Li}_2\text{CO}_3$)	phosphor 11 ($\text{SrCO}_3, \text{CaCO}_3, \text{Al}_2\text{O}_3, \text{Eu}_2\text{O}_3, \text{Dy}_2\text{O}_3, \text{H}_3\text{BO}_3, \text{SiO}_2, \text{Li}_2\text{CO}_3$)
		phosphor 1 ($\text{Sr}_4\text{Al}_{14}\text{O}_{25}:\text{Eu}^{3+}, \text{Dy}^{3+}$)	phosphor 2 ($\text{CaAl}_2\text{O}_4:\text{Eu}^{2+}, \text{Dy}^{3+}$)	phosphor 3 ($\text{SrCO}_3, \text{CaCO}_3, \text{Al}_2\text{O}_3, \text{Eu}_2\text{O}_3, \text{Dy}_2\text{O}_3, \text{H}_3\text{BO}_3, \text{SiO}_2, \text{Li}_2\text{CO}_3$)	phosphor 4 ($\text{SrCO}_3, \text{CaCO}_3, \text{Al}_2\text{O}_3, \text{Eu}_2\text{O}_3, \text{Dy}_2\text{O}_3, \text{H}_3\text{BO}_3, \text{SiO}_2, \text{Li}_2\text{CO}_3$)	phosphor 5 ($\text{SrCO}_3, \text{CaCO}_3, \text{Al}_2\text{O}_3, \text{Eu}_2\text{O}_3, \text{Dy}_2\text{O}_3, \text{H}_3\text{BO}_3, \text{SiO}_2, \text{Li}_2\text{CO}_3$)	phosphor 6 ($\text{SrCO}_3, \text{CaCO}_3, \text{Al}_2\text{O}_3, \text{Eu}_2\text{O}_3, \text{Dy}_2\text{O}_3, \text{H}_3\text{BO}_3, \text{SiO}_2, \text{Li}_2\text{CO}_3$)	phosphor 7 ($\text{SrCO}_3, \text{CaCO}_3, \text{Al}_2\text{O}_3, \text{Eu}_2\text{O}_3, \text{Dy}_2\text{O}_3, \text{H}_3\text{BO}_3, \text{SiO}_2, \text{Li}_2\text{CO}_3$)	phosphor 8 ($\text{SrCO}_3, \text{CaCO}_3, \text{Al}_2\text{O}_3, \text{Eu}_2\text{O}_3, \text{Dy}_2\text{O}_3, \text{H}_3\text{BO}_3, \text{SiO}_2, \text{Li}_2\text{CO}_3$)	phosphor 9 ($\text{SrCO}_3, \text{CaCO}_3, \text{Al}_2\text{O}_3, \text{Eu}_2\text{O}_3, \text{Dy}_2\text{O}_3, \text{H}_3\text{BO}_3, \text{SiO}_2, \text{Li}_2\text{CO}_3$)	phosphor 10 ($\text{SrCO}_3, \text{CaCO}_3, \text{Al}_2\text{O}_3, \text{Eu}_2\text{O}_3, \text{Dy}_2\text{O}_3, \text{H}_3\text{BO}_3, \text{SiO}_2, \text{Li}_2\text{CO}_3$)	phosphor 11 ($\text{SrCO}_3, \text{CaCO}_3, \text{Al}_2\text{O}_3, \text{Eu}_2\text{O}_3, \text{Dy}_2\text{O}_3, \text{H}_3\text{BO}_3, \text{SiO}_2, \text{Li}_2\text{CO}_3$)
		phosphor 1 ($\text{Sr}_4\text{Al}_{14}\text{O}_{25}:\text{Eu}^{3+}, \text{Dy}^{3+}$)	phosphor 2 ($\text{CaAl}_2\text{O}_4:\text{Eu}^{2+}, \text{Dy}^{3+}$)	phosphor 3 ($\text{SrCO}_3, \text{CaCO}_3, \text{Al}_2\text{O}_3, \text{Eu}_2\text{O}_3, \text{Dy}_2\text{O}_3, \text{H}_3\text{BO}_3, \text{SiO}_2, \text{Li}_2\text{CO}_3$)	phosphor 4 ($\text{SrCO}_3, \text{CaCO}_3, \text{Al}_2\text{O}_3, \text{Eu}_2\text{O}_3, \text{Dy}_2\text{O}_3, \text{H}_3\text{BO}_3, \text{SiO}_2, \text{Li}_2\text{CO}_3$)	phosphor 5 ($\text{SrCO}_3, \text{CaCO}_3, \text{Al}_2\text{O}_3, \text{Eu}_2\text{O}_3, \text{Dy}_2\text{O}_3, \text{H}_3\text{BO}_3, \text{SiO}_2, \text{Li}_2\text{CO}_3$)	phosphor 6 ($\text{SrCO}_3, \text{CaCO}_3, \text{Al}_2\text{O}_3, \text{Eu}_2\text{O}_3, \text{Dy}_2\text{O}_3, \text{H}_3\text{BO}_3, \text{SiO}_2, \text{Li}_2\text{CO}_3$)	phosphor 7 ($\text{SrCO}_3, \text{CaCO}_3, \text{Al}_2\text{O}_3, \text{Eu}_2\text{O}_3, \text{Dy}_2\text{O}_3, \text{H}_3\text{BO}_3, \text{SiO}_2, \text{Li}_2\text{CO}_3$)	phosphor 8 ($\text{SrCO}_3, \text{CaCO}_3, \text{Al}_2\text{O}_3, \text{Eu}_2\text{O}_3, \text{Dy}_2\text{O}_3, \text{H}_3\text{BO}_3, \text{SiO}_2, \text{Li}_2\text{CO}_3$)	phosphor 9 ($\text{SrCO}_3, \text{CaCO}_3, \text{Al}_2\text{O}_3, \text{Eu}_2\text{O}_3, \text{Dy}_2\text{O}_3, \text{H}_3\text{BO}_3, \text{SiO}_2, \text{Li}_2\text{CO}_3$)	phosphor 10 ($\text{SrCO}_3, \text{CaCO}_3, \text{Al}_2\text{O}_3, \text{Eu}_2\text{O}_3, \text{Dy}_2\text{O}_3, \text{H}_3\text{BO}_3, \text{SiO}_2, \text{Li}_2\text{CO}_3$)	phosphor 11 ($\text{SrCO}_3, \text{CaCO}_3, \text{Al}_2\text{O}_3, \text{Eu}_2\text{O}_3, \text{Dy}_2\text{O}_3, \text{H}_3\text{BO}_3, \text{SiO}_2, \text{Li}_2\text{CO}_3$)
phosphor mixing after a high-temperature solid-state reaction	green and blue phosphors mixing	phosphor 1 ($\text{SrAl}_2\text{O}_4:\text{Eu}^{2+}, \text{Dy}^{3+}$)	phosphor 2 ($\text{Sr}_4\text{Al}_{14}\text{O}_{25}:\text{Eu}^{3+}, \text{Dy}^{3+}$)	phosphor 3 ($\text{SrCO}_3, \text{CaCO}_3, \text{Al}_2\text{O}_3, \text{Eu}_2\text{O}_3, \text{Dy}_2\text{O}_3, \text{H}_3\text{BO}_3, \text{SiO}_2, \text{Li}_2\text{CO}_3$)	phosphor 4 ($\text{SrCO}_3, \text{CaCO}_3, \text{Al}_2\text{O}_3, \text{Eu}_2\text{O}_3, \text{Dy}_2\text{O}_3, \text{H}_3\text{BO}_3, \text{SiO}_2, \text{Li}_2\text{CO}_3$)	phosphor 5 ($\text{SrCO}_3, \text{CaCO}_3, \text{Al}_2\text{O}_3, \text{Eu}_2\text{O}_3, \text{Dy}_2\text{O}_3, \text{H}_3\text{BO}_3, \text{SiO}_2, \text{Li}_2\text{CO}_3$)	phosphor 6 ($\text{SrCO}_3, \text{CaCO}_3, \text{Al}_2\text{O}_3, \text{Eu}_2\text{O}_3, \text{Dy}_2\text{O}_3, \text{H}_3\text{BO}_3, \text{SiO}_2, \text{Li}_2\text{CO}_3$)	phosphor 7 ($\text{SrCO}_3, \text{CaCO}_3, \text{Al}_2\text{O}_3, \text{Eu}_2\text{O}_3, \text{Dy}_2\text{O}_3, \text{H}_3\text{BO}_3, \text{SiO}_2, \text{Li}_2\text{CO}_3$)	phosphor 8 ($\text{SrCO}_3, \text{CaCO}_3, \text{Al}_2\text{O}_3, \text{Eu}_2\text{O}_3, \text{Dy}_2\text{O}_3, \text{H}_3\text{BO}_3, \text{SiO}_2, \text{Li}_2\text{CO}_3$)	phosphor 9 ($\text{SrCO}_3, \text{CaCO}_3, \text{Al}_2\text{O}_3, \text{Eu}_2\text{O}_3, \text{Dy}_2\text{O}_3, \text{H}_3\text{BO}_3, \text{SiO}_2, \text{Li}_2\text{CO}_3$)	phosphor 10 ($\text{SrCO}_3, \text{CaCO}_3, \text{Al}_2\text{O}_3, \text{Eu}_2\text{O}_3, \text{Dy}_2\text{O}_3, \text{H}_3\text{BO}_3, \text{SiO}_2, \text{Li}_2\text{CO}_3$)	phosphor 11 ($\text{SrCO}_3, \text{CaCO}_3, \text{Al}_2\text{O}_3, \text{Eu}_2\text{O}_3, \text{Dy}_2\text{O}_3, \text{H}_3\text{BO}_3, \text{SiO}_2, \text{Li}_2\text{CO}_3$)
		phosphor 1 ($\text{Sr}_4\text{Al}_{14}\text{O}_{25}:\text{Eu}^{3+}, \text{Dy}^{3+}$)	phosphor 2 ($\text{CaAl}_2\text{O}_4:\text{Eu}^{2+}, \text{Dy}^{3+}$)	phosphor 3 ($\text{SrCO}_3, \text{CaCO}_3, \text{Al}_2\text{O}_3, \text{Eu}_2\text{O}_3, \text{Dy}_2\text{O}_3, \text{H}_3\text{BO}_3, \text{SiO}_2, \text{Li}_2\text{CO}_3$)	phosphor 4 ($\text{SrCO}_3, \text{CaCO}_3, \text{Al}_2\text{O}_3, \text{Eu}_2\text{O}_3, \text{Dy}_2\text{O}_3, \text{H}_3\text{BO}_3, \text{SiO}_2, \text{Li}_2\text{CO}_3$)	phosphor 5 ($\text{SrCO}_3, \text{CaCO}_3, \text{Al}_2\text{O}_3, \text{Eu}_2\text{O}_3, \text{Dy}_2\text{O}_3, \text{H}_3\text{BO}_3, \text{SiO}_2, \text{Li}_2\text{CO}_3$)	phosphor 6 ($\text{SrCO}_3, \text{CaCO}_3, \text{Al}_2\text{O}_3, \text{Eu}_2\text{O}_3, \text{Dy}_2\text{O}_3, \text{H}_3\text{BO}_3, \text{SiO}_2, \text{Li}_2\text{CO}_3$)	phosphor 7 ($\text{SrCO}_3, \text{CaCO}_3, \text{Al}_2\text{O}_3, \text{Eu}_2\text{O}_3, \text{Dy}_2\text{O}_3, \text{H}_3\text{BO}_3, \text{SiO}_2, \text{Li}_2\text{CO}_3$)	phosphor 8 ($\text{SrCO}_3, \text{CaCO}_3, \text{Al}_2\text{O}_3, \text{Eu}_2\text{O}_3, \text{Dy}_2\text{O}_3, \text{H}_3\text{BO}_3, \text{SiO}_2, \text{Li}_2\text{CO}_3$)	phosphor 9 ($\text{SrCO}_3, \text{CaCO}_3, \text{Al}_2\text{O}_3, \text{Eu}_2\text{O}_3, \text{Dy}_2\text{O}_3, \text{H}_3\text{BO}_3, \text{SiO}_2, \text{Li}_2\text{CO}_3$)	phosphor 10 ($\text{SrCO}_3, \text{CaCO}_3, \text{Al}_2\text{O}_3, \text{Eu}_2\text{O}_3, \text{Dy}_2\text{O}_3, \text{H}_3\text{BO}_3, \text{SiO}_2, \text{Li}_2\text{CO}_3$)	phosphor 11 ($\text{SrCO}_3, \text{CaCO}_3, \text{Al}_2\text{O}_3, \text{Eu}_2\text{O}_3, \text{Dy}_2\text{O}_3, \text{H}_3\text{BO}_3, \text{SiO}_2, \text{Li}_2\text{CO}_3$)

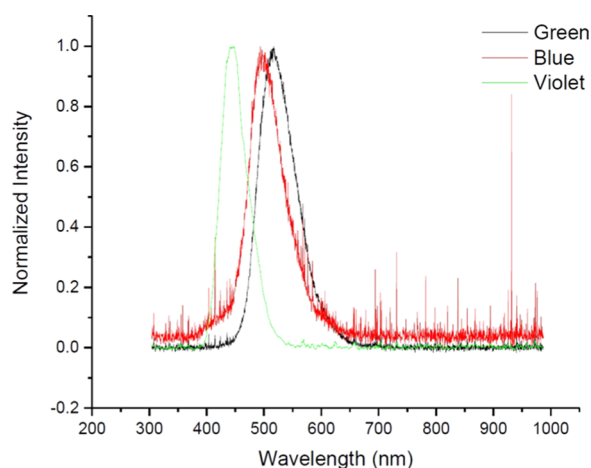


Figure 2. Emission spectrum of alkaline-earth aluminate ($\text{SrAl}_2\text{O}_4:\text{Eu}^{2+}$, Dy^{3+} and $\text{Sr}_4\text{Al}_{14}\text{O}_{25}:\text{Eu}^{2+}$, Dy^{3+}) and calcium aluminate phosphors ($\text{CaAl}_2\text{O}_4:\text{Eu}^{2+}$, Nd^{3+}) as the green, blue, and violet phosphors, respectively.

important for enhancing the afterglow intensity and increasing the decay time.

The energy transfer effect from the violet to blue phosphor was examined based on the previous result. In the same

manner as the previous experiment, the blue ($\text{Sr}_4\text{Al}_{14}\text{O}_{25}:\text{Eu}^{2+}$, Dy^{3+}) and violet ($\text{CaAl}_2\text{O}_4:\text{Eu}^{2+}$, Nd^{3+}) phosphors were mixed in ratios ranging from 9:1 to 5:5, as shown in Table 1, to enhance the phosphorescence of the blue phosphor ($\text{Sr}_4\text{Al}_{14}\text{O}_{25}:\text{Eu}^{2+}$, Dy^{3+}). Subsequently, the mixed powders were fired in horizontal tube furnaces for the high-temperature solid-state reaction. An emission band of all of the materials was observed at 448 nm, corresponding to the phosphorescence wavelength of the blue phosphor.¹ The blue phosphor acted as an acceptor, whereas the violet phosphor acted as a donor during the energy transfer process. To measure the afterglow intensity of the blue phosphor, the emission peak at ~ 448 nm was monitored as it corresponds to the $5d \rightarrow 4f$ transition in Eu^{2+} ions.¹ Figure 4 shows that the initial afterglow intensity measured at 5 s changed significantly as a function of the B:V molar ratio, consistent with the afterglow intensity of the G:B mixture. The increased phosphorescence intensity upon mixing the blue and violet phosphors varied from 150 to 34 400% of the initial value. In contrast to the green and blue phosphor mixture, the initial afterglow intensity began to decrease when the B:V ratio reached 5:5. The emission spectrum of the B:V = 5:5 sample was similar to that of the violet phosphor, indicating that the emission center of this sample moved to the violet region, decreasing the blue emission (Table 3). Therefore, energy transfer from the violet

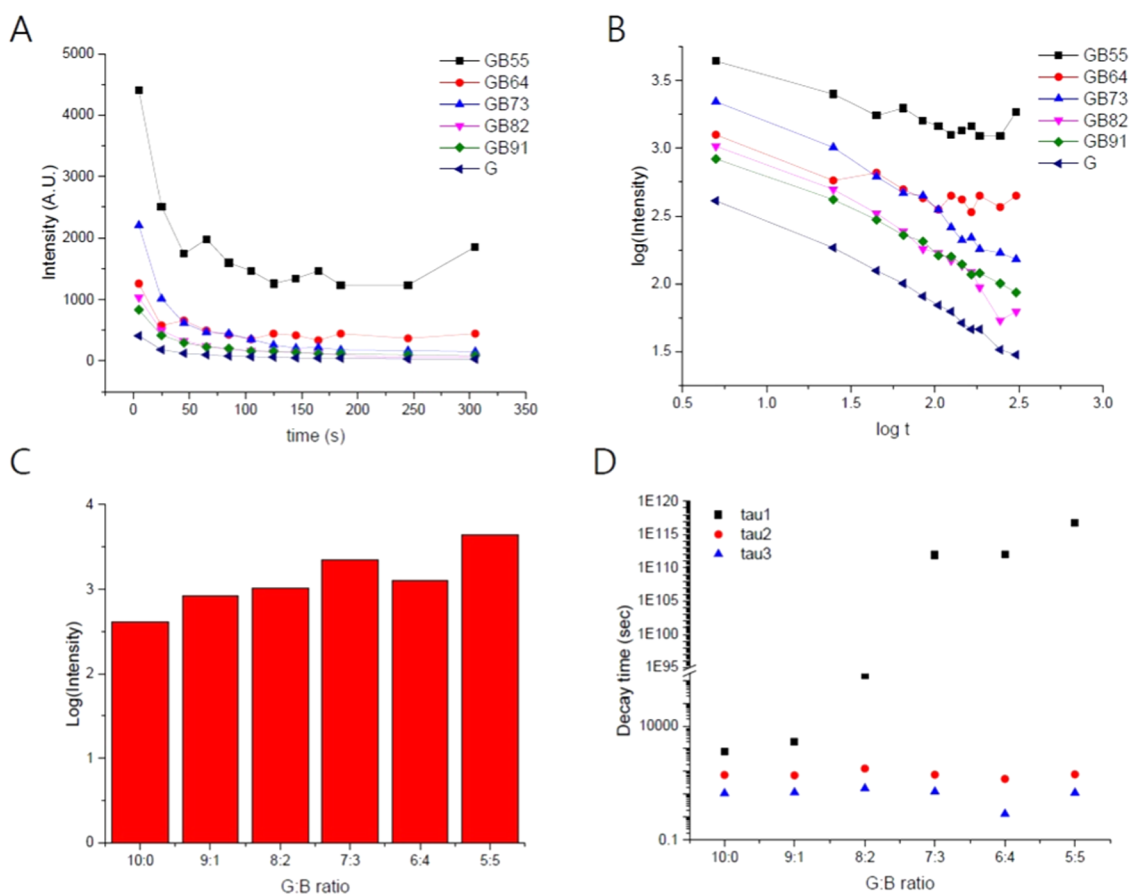
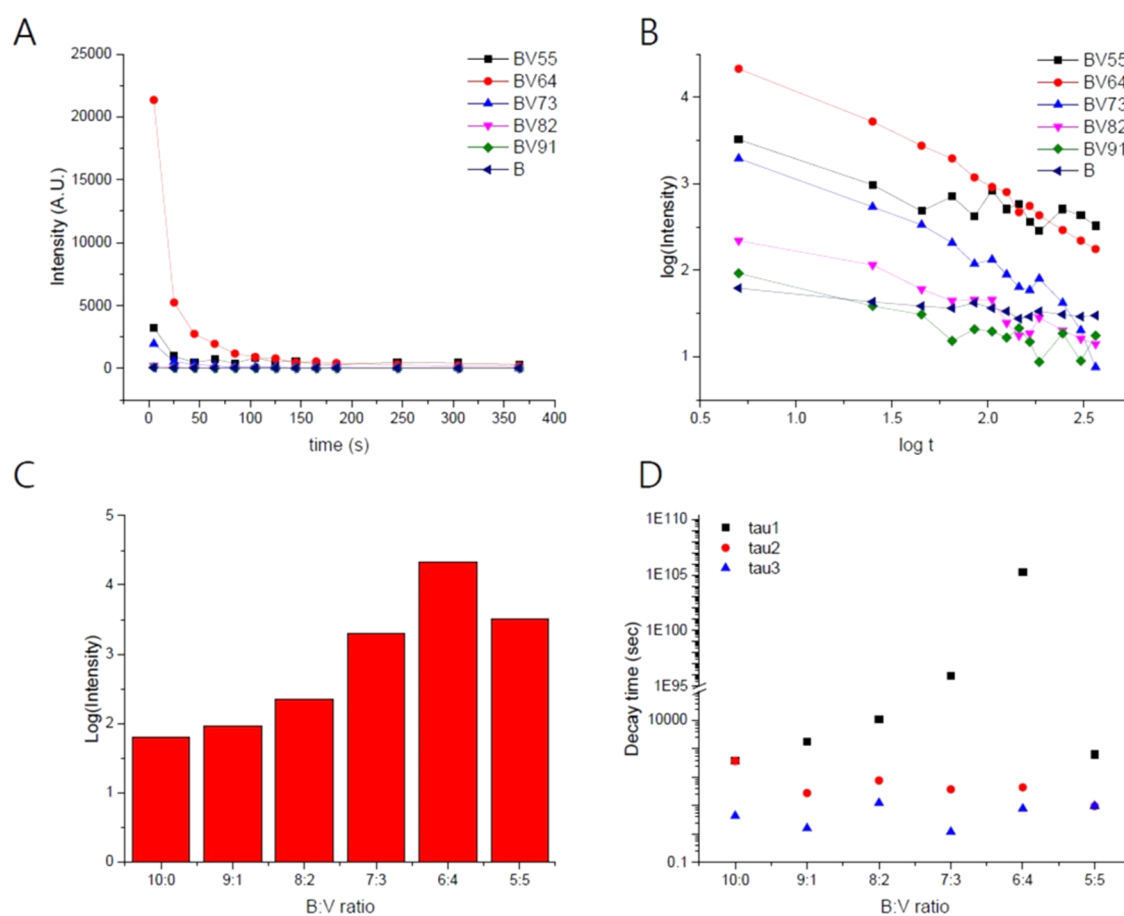


Figure 3. (A) Decay curves for samples with various green phosphor:blue phosphor (G:B) molar ratios of 10:0–5:5 synthesized by chemical mixing before high-temperature solid-state reaction. (B) Decay curves in log scale for samples with various G:B ratios synthesized by chemical mixing before high-temperature solid-state reaction. (C) Initial intensity measured at 5 s for samples with various G:B molar ratios ranging from 10:0 to 5:5, synthesized by chemical mixing before high-temperature solid-state reaction. (D) Calculated phosphorescence decay times from the samples with various green phosphor:blue phosphor (G:B) molar ratios of 10:0–5:5 synthesized by chemical mixing before high-temperature solid-state reaction.

Table 2. Calculated Phosphorescence Decay Times from the Green and Blue Phosphor Mixtures Synthesized by Chemical Mixing before High-Temperature Solid-State Reaction Obtained from the Three Exponential Components by Curve Fitting^a

G:B	10:0	9:1	8:2	7:3	6:4	5:5
t_1 [s]	7.585×10^2	2.097×10^3	1.780×10^6	8.563×10^{11}	9.291×10^{11}	5.428×10^{16}
t_2 [s]	7.013×10^1	6.765×10^1	1.342×10^2	7.251×10^1	4.715×10^1	7.458×10^1
t_3 [s]	1.109×10^1	1.209×10^1	1.815×10^1	1.305×10^1	1.376×10^0	1.162×10^1
A_1	4.119×10^1	1.027×10^2	3.136×10^1	1.299×10^2	3.904×10^2	1.175×10^3
A_2	1.530×10^2	3.460×10^2	2.900×10^2	8.391×10^2	4.099×10^2	1.294×10^3
A_3	3.553×10^2	6.223×10^2	9.659×10^2	1.899×10^3	1.893×10^4	3.109×10^3

$$^a I = A_1 e^{-t/t_1} + A_2 e^{-t/t_2} + A_3 e^{-t/t_3}$$

**Figure 4.** (A) Decay curves for samples with various blue phosphor:violet phosphor (B:V) molar ratios of 10:0–5:5 synthesized by chemical mixing before high-temperature solid-state reaction. (B) Decay curves in log scale for samples with various B:V ratios synthesized by chemical mixing before high-temperature solid-state reaction. (C) Initial intensity measured at 5 s for samples with various B:V molar ratios ranging from 10:0 to 5:5, synthesized by chemical mixing before high-temperature solid-state reaction. (D) Calculated phosphorescence decay times from the samples with various blue phosphor:violet phosphor (B:V) molar ratios of 10:0–5:5 synthesized by chemical mixing before high-temperature solid-state reaction.**Table 3. Calculated Phosphorescence Decay Times from the Blue and Violet Phosphor Mixtures Synthesized by Chemical Mixing before High-Temperature Solid-State Reaction Obtained from the Three Exponential Components by Curve Fitting^a**

B:V	10:0	9:1	8:2	7:3	6:4	5:5
t_1 [s]	3.705×10^2	1.709×10^3	1.088×10^4	8.797×10^{95}	1.961×10^{105}	6.261×10^2
t_2 [s]	3.678×10^2	2.729×10^1	7.552×10^1	3.699×10^1	4.343×10^1	9.527×10^0
t_3 [s]	4.322×10^0	1.571×10^0	1.234×10^1	1.183×10^0	7.760×10^0	9.525×10^0
A_1	3.417×10^1	1.720×10^1	1.488×10^1	4.725×10^1	3.402×10^2	6.438×10^2
A_2	1.172×10^1	5.514×10^1	7.857×10^1	9.632×10^2	6.674×10^3	2.833×10^3
A_3	5.319×10^1	6.960×10^2	2.326×10^2	7.337×10^4	2.868×10^4	1.588×10^3

$$^a I = A_1 e^{-t/t_1} + A_2 e^{-t/t_2} + A_3 e^{-t/t_3}$$

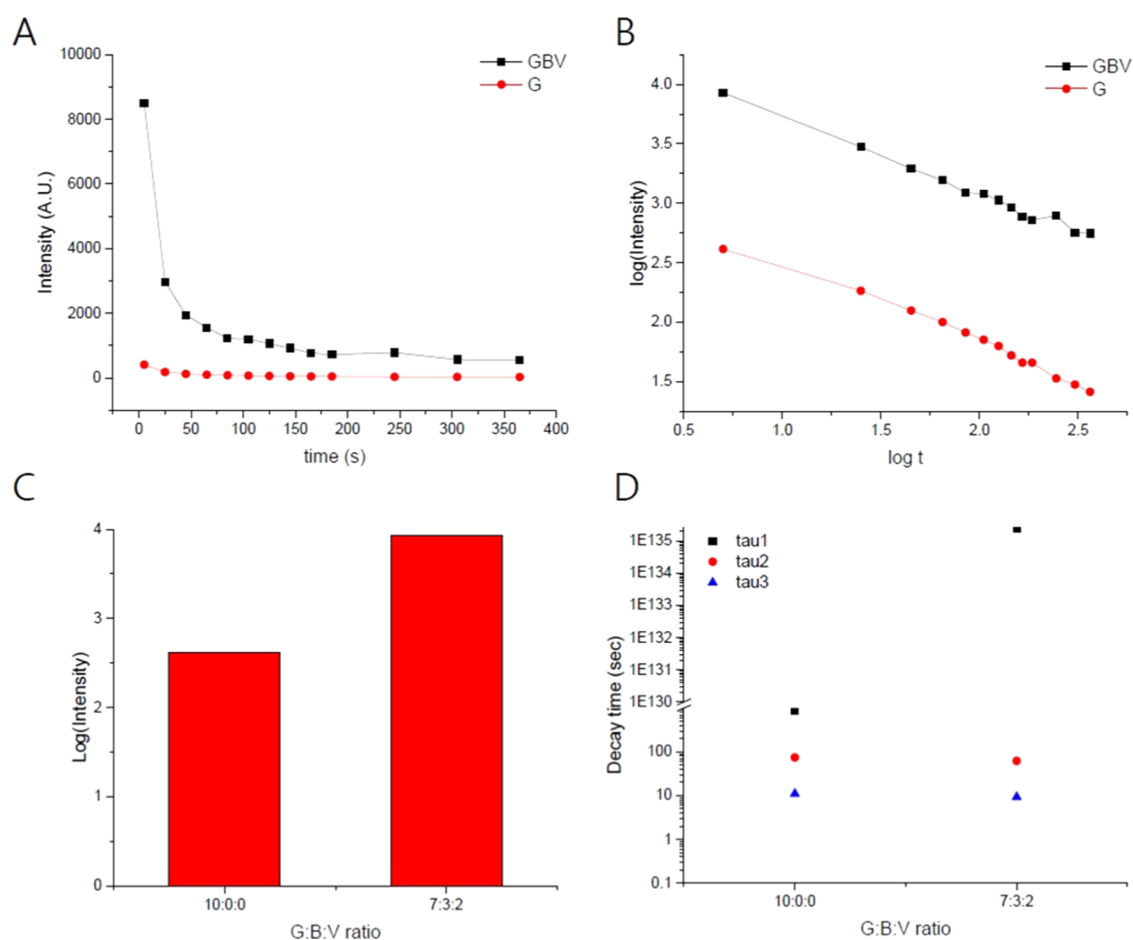


Figure 5. (A) Decay curves for samples with various green phosphor:blue phosphor:violet phosphor (G:B:V) molar ratios of 10:0:0–7:3:2 synthesized by chemical mixing before high-temperature solid-state reaction. (B) Decay curves in log scale for samples with various G:B:V ratios synthesized by chemical mixing before high-temperature solid-state reaction. (C) Initial intensity measured at 5 s for samples with various G:B:V molar ratios ranging from 10:0:0 to 7:3:2, synthesized by chemical mixing before high-temperature solid-state reaction. (D) Calculated phosphorescence decay times from the samples with various green phosphor:blue phosphor:violet phosphor (G:B:V) molar ratios of 10:0–5:5 synthesized by chemical mixing before high-temperature solid-state reaction.

to blue phosphor is likely to enhance the afterglow intensity of the violet phosphor in a similar manner to that from the blue to green phosphor up to a B:V ratio of 6:4.

The multistep energy transfer from the violet to green phosphor was further investigated in conjunction with the blue phosphor, which has not been reported to date, to the best of our knowledge. If the energy is successfully transferred from the violet to blue phosphor in the first step, and from the blue to green phosphor in the next step as observed previously, an efficient energy transfer from the violet to green phosphor should be observed with increased phosphorescence intensity and longer lifetime of the green phosphor. To achieve this multistep energy transfer effect, the green ($\text{SrAl}_2\text{O}_4\text{:Eu}^{2+}$, Dy^{3+}), blue ($\text{Sr}_4\text{Al}_{14}\text{O}_{25}\text{:Eu}^{2+}$, Dy^{3+}), and violet ($\text{CaAl}_2\text{O}_4\text{:Eu}^{2+}$, Nd^{3+}) phosphors were mixed in a ratio of 7:3:2, as shown in Table 1, and subsequently fired in horizontal tube furnaces for the high-temperature solid-state reaction (Figure 5 and Table 4). It was apparent that the afterglow intensity of the green phosphor was significantly enhanced by chemical mixing with the blue and violet phosphors. Thus, the increased phosphorescence intensity of the green phosphor from mixing with the blue phosphor was enhanced by chemical mixing with the blue and violet phosphors, as shown in Figure 5. The phosphor mixture at a ratio of 7:3:2 also significantly increased

Table 4. Calculated Phosphorescence Decay Times from the Green, Blue, and Violet Phosphor Mixtures Synthesized by Chemical Mixing before High-Temperature Solid-State Reaction Obtained from the Three Exponential Components by Curve Fitting^a

G:B:V	10:0:0	7:3:2
t_1 [s]	3.636×10^2	2.536×10^{135}
t_2 [s]	1.519×10^2	6.163×10^1
t_3 [s]	1.106×10^1	9.303×10^0
A_1	7.397×10^1	6.732×10^2
A_2	8.644×10^2	2.487×10^3
A_3	3.810×10^1	9.485×10^3

$$^a I = A_1 e^{1/t_1} + A_2 e^{1/t_2} + A_3 e^{1/t_3}$$

the decay time, as shown in Table 4 and Figure 5D, which is much longer than those of previously tested green and blue phosphor mixtures. This observation indicates that the energy transfer can be further enhanced by multistep energy transfer.

Chemical Mixing of Two Different Phosphors by Firing after High-Temperature Solid-State Reactions of Each Phosphor. In this approach, the starting materials of each phosphor (green ($\text{SrAl}_2\text{O}_4\text{:Eu}^{2+}$, Dy^{3+}) and blue ($\text{Sr}_4\text{Al}_{14}\text{O}_{25}\text{:Eu}^{2+}$, Dy^{3+}) phosphors, or blue ($\text{Sr}_4\text{Al}_{14}\text{O}_{25}\text{:Eu}^{2+}$,

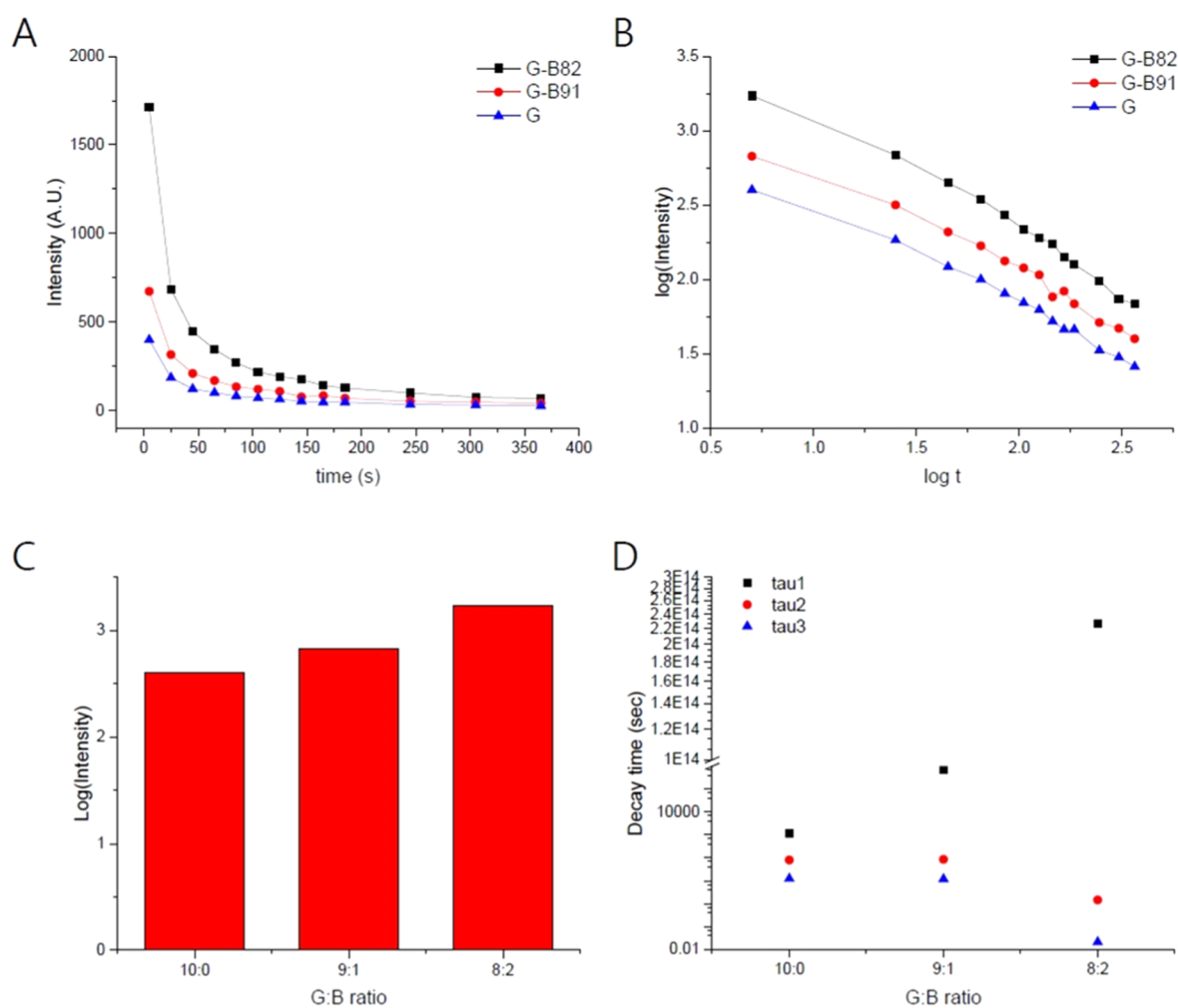


Figure 6. (A) Decay curves for samples with various green phosphor:blue phosphor (G:B) molar ratios of 10:0–8:2 synthesized by chemical mixing after high-temperature solid-state reaction. (B) Decay curves in log scale for samples with various G:B ratios synthesized by chemical mixing after high-temperature solid-state reaction. (C) Initial intensity measured at 5 s for samples with various G:B molar ratios ranging from 10:0 to 8:2, synthesized by chemical mixing after high-temperature solid-state reaction. (D) Calculated phosphorescence decay times from the samples with various green phosphor:blue phosphor (G:B) molar ratios of 10:0–8:2 synthesized by chemical mixing after high-temperature solid-state reaction.

Dy³⁺) and violet (CaAl₂O₄:Eu²⁺, Nd³⁺) phosphors) were mixed, respectively, as shown in Table 1, and synthesized separately via a high-temperature solid-state reaction.^{1,13} Subsequently, the different phosphors were mixed at ratios ranging from 10:0 to 8:2 using an agate mortar and subsequently fired in the presence of H₃BO₃ at 800–1400 °C. After cooling the samples, their emission spectra were measured at room temperature. The phosphorescence properties of the samples are shown in Figure 6 and Table 5, including the initial afterglow intensity measured at 5 s and decay times calculated from the fitting with three exponential components.

After chemical mixing of the green and blue phosphors, the afterglow intensity was monitored at the ~520 nm emission peak to investigate the energy transfer effect between the separately synthesized phosphors because the peak of the emission spectrum of the green phosphor (SrAl₂O₄:Eu²⁺) is observed at 520 nm from the 4f → 5d transition of Eu²⁺. Figure 6 shows the decay curves for the phosphors synthesized with different ratios of green and blue phosphors. The initial afterglow intensity of the green phosphor measured at 5 s increased upon addition of the blue phosphor, as shown in Figure 6C, indicating that the energy of the blue phosphor was

Table 5. Calculated Phosphorescence Decay Times from the Green and Blue Phosphor Mixtures Synthesized by Chemical Mixing after High-Temperature Solid-State Reaction Obtained from the Three Exponential Components by Curve Fitting^a

G:B	10:0	9:1	8:2
t_1 [s]	3.483×10^2	5.909×10^2	2.262×10^{14}
t_2 [s]	1.415×10^2	2.689×10^2	7.739×10^8
t_3 [s]	1.247×10^1	1.200×10^1	2.546×10^2
A_1	8.228×10^1	8.702×10^1	4.083×10^4
A_2	1.193×10^3	7.191×10^5	1.460×10^0
A_3	3.333×10^1	3.676×10^1	2.092×10^{-2}

$$^a I = A_1 e^{-t/t_1} + A_2 e^{-t/t_2} + A_3 e^{-t/t_3}$$

successfully transferred to the green phosphor. In the same manner as the phosphorescence intensity, the increase of decay time (Table 5) with the increase of the relative amount of blue phosphor indicates the effective energy transfer from the green to blue phosphor.

Next, the chemical mixing of the blue and violet phosphors by firing after high-temperature solid-state reactions of each phosphor was performed to enhance the luminescence of the

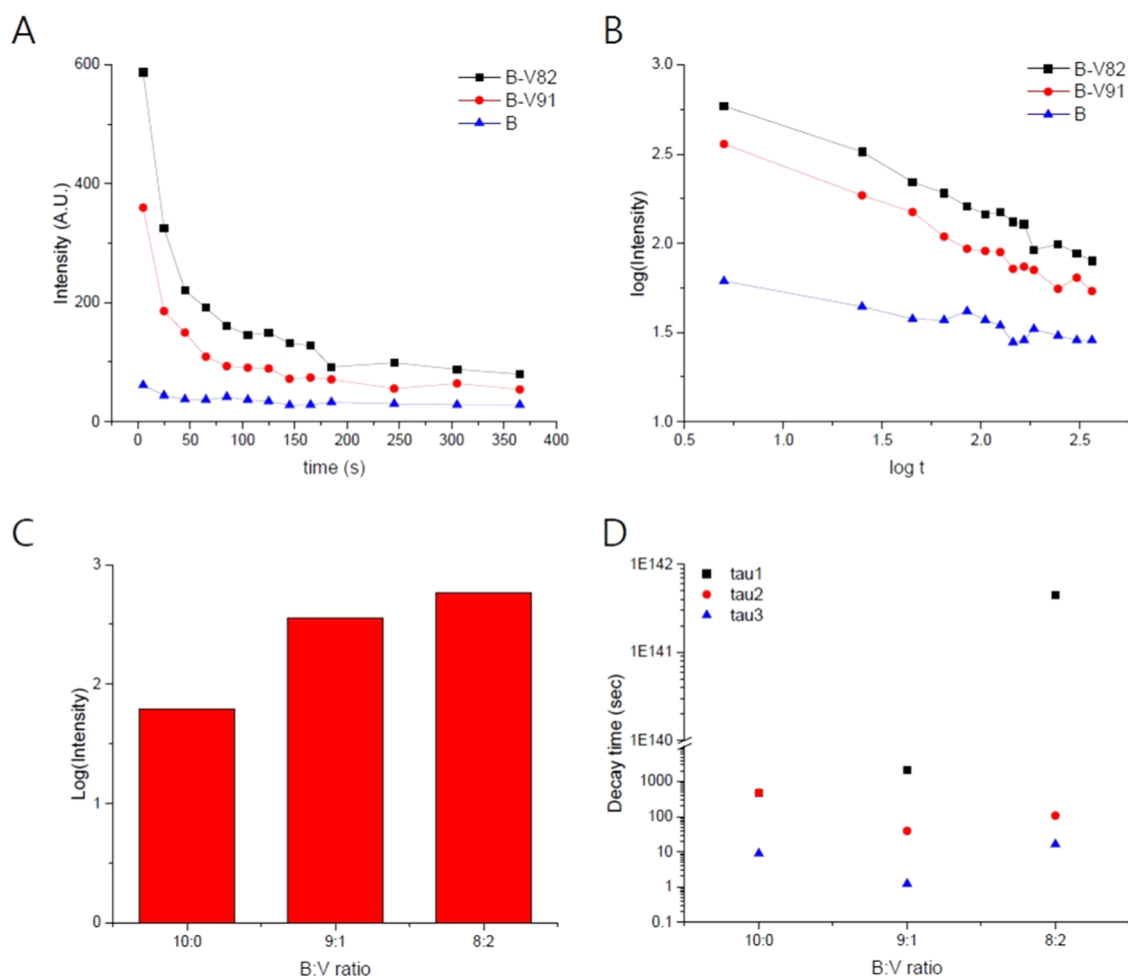


Figure 7. (A) Decay curves for samples with various blue phosphor:violet phosphor (B:V) molar ratios of 10:0–8:2 synthesized by chemical mixing after high-temperature solid-state reaction. (B) Decay curves in log scale for samples with various B:V ratios synthesized by chemical mixing after high-temperature solid-state reaction. (C) Initial intensity measured at 5 s for samples with various B:V molar ratios ranging from 10:0 to 8:2, synthesized by chemical mixing after high-temperature solid-state reaction. (D) Calculated phosphorescence decay times from the samples with various blue phosphor:violet phosphor (B:V) molar ratios of 10:0–8:2 synthesized by chemical mixing after high-temperature solid-state reaction.

blue phosphor. The mixtures of the phosphors were synthesized by mixing in various ratios, as shown in Table 1, and the measured and calculated photophysical results are listed in Figure 7 and Table 6. A >10 times increased luminescence of the blue phosphor relative to that of the control sample was achieved by chemical mixing with violet phosphor. This increase is larger than the phosphorescence increase of the green–blue phosphor, indicating that the

energy transfer from the violet to blue phosphor is more efficient than that from the blue to green phosphor.

The results from the two chemical mixing approaches were compared (mixed before or after the high-temperature solid-state reaction). The phosphorescence intensity increased more significantly using the second approach (chemical mixing after high-temperature solid-state reaction) compared to that using the first approach (chemical mixing before high-temperature solid-state reaction), diverging from expectations. It was expected that the energy would be transferred more effectively using the first approach because the distance between the spectrally different phosphors is shorter. However, the results showed that phosphorescence can be enhanced more effectively using the second approach probably due to a higher energy transfer rate. The results can be explained by unoptimized concentrations for each of the spectrally different phosphors when mixed before the high-temperature solid-state reaction in the first approach. It can be also explained by different crystal field distortion effects followed by different phosphorescence mechanisms between two approaches because it is known that crystal field distortion affects the f – d transitions significantly.²⁶ In contrast to the first approach, in the second approach, each spectrally different phosphor can be

Table 6. Calculated Phosphorescence Decay Times from the Blue and Violet Phosphor Mixtures Synthesized by Chemical Mixing after High-Temperature Solid-State Reaction Obtained from the Three Exponential Components by Curve Fitting^a

B:V	10:0	9:1	8:2
t_1 [s]	4.822×10^2	2.129×10^3	4.485×10^{141}
t_2 [s]	4.817×10^2	3.924×10^1	1.066×10^2
t_3 [s]	8.852×10^0	1.208×10^0	1.625×10^1
A_1	2.357×10^1	7.685×10^1	7.982×10^1
A_2	2.025×10^1	2.112×10^2	1.828×10^2
A_3	3.160×10^1	6.102×10^3	4.536×10^2

$$^a I = A_1 e^{-t/t_1} + A_2 e^{-t/t_2} + A_3 e^{-t/t_3}$$

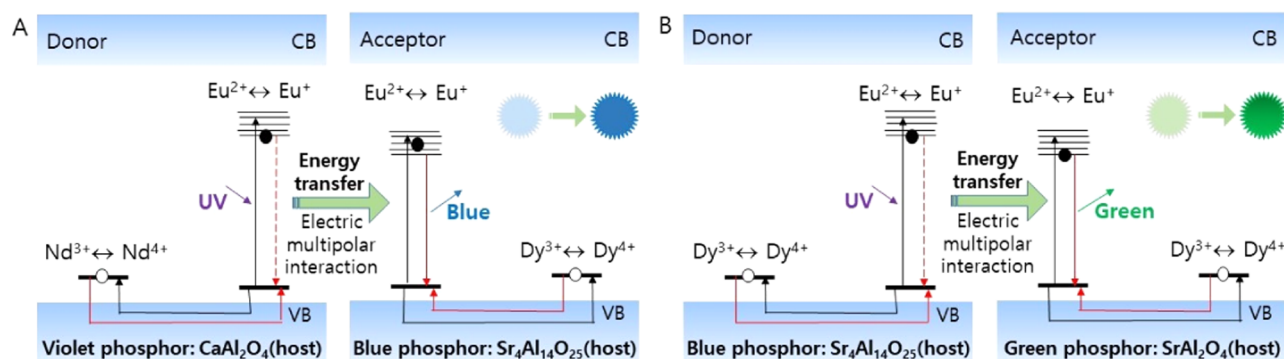


Figure 8. Schematic of the energy transfer process between the donor and acceptor ions in different host materials. (A) Simplified energy transfer model in violet–blue phosphor mixing. (B) Simplified energy transfer model in blue–green phosphor mixing.

optimally synthesized using separate reactions and subsequently mixed, allowing for more efficient energy transfer.

DISCUSSION

Herein, we systematically investigated the energy transfer between spectrally different phosphors with the aim of developing bright and long-persistent green and blue phosphors. Alkaline-earth aluminate ($\text{SrAl}_2\text{O}_4\text{:Eu}^{2+}$, Dy^{3+} and $\text{Sr}_4\text{Al}_{14}\text{O}_{25}\text{:Eu}^{2+}$, Dy^{3+}) and calcium aluminate phosphors ($\text{CaAl}_2\text{O}_4\text{:Eu}^{2+}$, Nd^{3+}) were used as green-, blue-, and violet-emitting phosphors, respectively. It was expected that the energy from the violet phosphor would be transferred to the blue phosphor and that from the blue phosphor would be transferred to the green phosphor depending on the spectral overlap between the phosphor pair. For an effective energy transfer between spectrally different phosphors, two chemical mixing methods were applied: mixing before high-temperature solid-state reaction and after each high-temperature solid-state reaction. The initial afterglow characteristics of the green and blue phosphors were improved when mixed with the relatively higher-energy phosphor regardless of the preparation approach. In particular, when the green and blue phosphors were mixed in a 5:5 ratio before the high-temperature solid-state reaction, the strongest persistent luminescence (1100% enhancement) was observed. The similar enhancement of persistent luminescence has been reported from the energy transfer from Ce^{3+} to Tb^{3+} in $\text{Ba-Lu}_6(\text{Si}_2\text{O}_7)_2(\text{Si}_3\text{O}_{10})\text{:Ce}^{3+}, \text{Tb}^{3+}$ (BLSO: $\text{Ce}^{3+}, \text{Tb}^{3+}$), in which the Tb^{3+} emission is greatly enhanced for about 10 times.²³ When the blue and violet phosphors were mixed in a 6:4 ratio before high-temperature solid-state reaction, the brightest and longest emission (34 400% enhancement) was observed. The persistent luminescence intensity of the green phosphor was further enhanced when it is co-mixed with the blue and violet phosphors (2100% enhancement) via a multistep energy transfer. Using chemical mixing after high-temperature solid-state reaction yielded an optimal green and blue phosphor ratio of 8:2, as it exhibited brighter and longest emission than those obtained using 9:1 mixture ratios and control samples. Therefore, it can be concluded that the chemical mixing approach can increase the phosphorescence intensity via energy transfer.

The dependence of the emission intensity of the acceptor phosphor on the concentration of the donor phosphor observed in this study is consistent with the observation from the previously reported studies on the energy transfer in single host materials. This is considered as strong evidence for

the energy transfer in phosphors. Although there are two possible energy transfer mechanisms for the resonant energy transfer, such as exchange interaction and multipolar interaction, the exchange interaction can be ruled out here as it often occurs when the critical distance between a donor and an acceptor is approximately 5 Å, which is much shorter than that in our case. Moreover, the energy transfer mechanism in previously reported phosphors has been determined to be a multipolar interaction including the dipole–dipole and dipole–quadrupole interactions, which is consistent with our conclusion.^{22,24} Therefore, electric multipolar interaction is suspected to be responsible for the energy transfer mechanism between Eu^{2+} ions in different host materials (Figure 8).

In conclusion, a promising and simple method for enhancing preexisting phosphorescence properties was developed herein. We expect that further studies utilizing different experimental spectroscopic and other microscopic techniques, such as XRD or SEM/TEM, would be valuable to characterize their structural and morphological properties. We anticipate that they will be valuable tools to understand the effect of morphology of the phosphors on the photoluminescence intensity of the materials and further establish the underlying mechanisms in detail. This protocol has the potential to be expanded to other fields that require different types of phosphors.

METHODS

For the chemical mixing of two or three different phosphors via high-temperature solid-state reaction, all starting materials were first weighed, mixed homogeneously, and subsequently ground using an agate mortar. The ground powder mixtures were fired in molybdenum crucibles under a weak reductive atmosphere of $\text{N}_2\text{--H}_2$ gas at ~ 1300 °C for 3–5 h. For chemical mixing of two different phosphors by firing after high-temperature solid-state reactions of each phosphor, the starting materials for each phosphor were first weighed and subsequently mixed and ground in an agate mortar separately. Afterward, each phosphor was synthesized separately via a high-temperature solid-state reaction and the separately synthesized phosphors were mixed at ratios of 10:0 or 5:5 in an agate mortar and fired in the presence of H_3BO_3 at 800–1400 °C. The synthesized powders were cooled to room temperature and ground again in an agate mortar. To measure the afterglow intensity, the samples were irradiated at 365 nm for 5 min. After irradiation, the emission spectrum of each sample was recorded using a Hitachi 850 fluorescence spectrophotometer from 300 to 950 nm at room temperature.

The decay curves from the measured spectra were fitted by three exponential components to calculate the lifetimes, which are the inverse decay rates.

AUTHOR INFORMATION

Corresponding Author

Doory Kim – Department of Chemistry, Research Institute for Convergence of Basic Sciences, and Institute of Nano Science and Technology, Hanyang University, Seoul 04763, South Korea;

orcid.org/0000-0002-2675-106X; Email: doorykim@hanyang.ac.kr

Authors

Han-Eol Kim – Gwangju Institute of Science and Technology, Gwangju 61005, South Korea

Chang-Hong Kim – Korea Institute of Science and Technology, Seoul 02792, South Korea

Complete contact information is available at:

<https://pubs.acs.org/10.1021/acsomega.0c00620>

Notes

The authors declare no competing financial interest.

ACKNOWLEDGMENTS

This work was supported by the research fund of Hanyang University (HY-2018).

REFERENCES

- (1) Matsuzawa, T.; Aoki, Y.; Takeuchi, N.; Murayama, Y. A New Long Phosphorescent Phosphor with High Brightness, SrAl₂O₄: Eu²⁺, Dy³⁺. *J. Electrochem. Soc.* **1996**, *143*, 2670–2673.
- (2) Palilla, F. C.; Levine, A. K.; Tomkus, M. R. Fluorescent Properties of Alkaline Earth Aluminates of the Type MAl₂O₄ Activated by Divalent Europium. *J. Electrochem. Soc.* **1968**, *115*, 642–644.
- (3) Kinoshita, T.; Yamazaki, M.; Kawazoe, H.; Hosono, H. Long lasting phosphorescence and photostimulated luminescence in Tb-ion-activated reduced calcium aluminate glasses. *J. Appl. Phys.* **1999**, *86*, 3729–3733.
- (4) Hölsä, J.; Jungner, H.; Lastusaari, M.; Niittykoski, J. Persistent luminescence of Eu²⁺ doped alkaline earth aluminates, MAl₂O₄: Eu²⁺. *J. Alloys Compd.* **2001**, *323–324*, 326–330.
- (5) Aitasalo, T.; Dereñ, P.; Hölsä, J.; Jungner, H.; Krupa, J.-C.; Lastusaari, M.; Legendziewicz, J.; Niittykoski, J.; Stręk, W. Persistent luminescence phenomena in materials doped with rare earth ions. *J. Solid State Chem.* **2003**, *171*, 114–122.
- (6) Clabau, F.; Rocquefelte, X.; Jobic, S.; Deniard, P.; Whangbo, M.-H.; Garcia, A.; Le, T. Mercier, Mechanism of phosphorescence appropriate for the long-lasting phosphors Eu²⁺-doped SrAl₂O₄ with codopants Dy³⁺ and B³⁺. *Chem. Mater.* **2005**, *17*, 3904–3912.
- (7) Zhai, B.-g.; Ma, Q.-l.; Xiong, R.; Li, X.; Huang, Y. M. Blue–green afterglow of BaAl₂O₄: Dy³⁺ phosphors. *Mater. Res. Bull.* **2016**, *75*, 1–6.
- (8) Yadav, R.; Rai, S.; Dhoble, S. Recent advances on morphological changes in chemically engineered rare earth doped phosphor materials. *Prog. Solid State Chem.* **2019**, No. 100267.
- (9) Jain, A.; Sengar, P.; Hirata, G. A. Rare-earth-doped Y₃Al₅O₁₂ (YAG) nanophosphors: synthesis, surface functionalization, and applications in thermoluminescence dosimetry and nanomedicine. *J. Phys. D: Appl. Phys.* **2018**, *51*, No. 303002.
- (10) Choudhary, A.; Dwivedi, A.; Bahadur, A.; Rai, S. Enhanced upconversion from Er³⁺/Yb³⁺ co-doped alkaline earth aluminates phosphor in presence Zn²⁺: A comparative study. *J. Lumin.* **2019**, *210*, 135–141.
- (11) Kim, D.; Kim, H.-E.; Kim, C.-H. Effect of composition and impurities on the phosphorescence of green-emitting alkaline earth aluminate phosphor. *PLoS One* **2016**, *11*, No. e0145434.
- (12) Kim, D.; Kim, H.-E.; Kim, C.-H. Development of a blue emitting calcium-aluminate phosphor. *PLoS One* **2016**, *11*, No. e0162920.
- (13) Yu, X.; Xu, X.; Zhou, C.; Tang, J.; Peng, X.; Yang, S. Synthesis and luminescent properties of SrZnO₂: Eu³⁺, M⁺ (M = Li, Na, K) phosphor. *Mater. Res. Bull.* **2006**, *41*, 1578–1583.
- (14) Prakashbabu, D.; Ramalingam, H.; Krishna, R. H.; Nagabhushana, B.; Chandramohan, R.; Shivakumara, C.; Thirumalai, J.; Thomas, T. Charge compensation assisted enhancement of photoluminescence in combustion derived Li⁺ co-doped cubic ZrO₂: Eu³⁺ nanophosphors. *Phys. Chem. Chem. Phys.* **2016**, *18*, 29447–29457.
- (15) Mindru, I.; Gingasu, D.; Patron, L.; Marinescu, G.; Calderon-Moreno, J. M.; Diamandescu, L.; Secu, M.; Oprea, O. Tb³⁺-doped alkaline-earth aluminates: Synthesis, characterization and optical properties. *Mater. Res. Bull.* **2017**, *85*, 240–248.
- (16) Rodrigues, L. C.; Hölsä, J.; Carvalho, J. M.; Pedroso, C. C.; Lastusaari, M.; Felinto, M. C.; Watanabe, S.; Brito, H. F. Co-dopant influence on the persistent luminescence of BaAl₂O₄: Eu²⁺, R³⁺. *Phys. B* **2014**, *439*, 67–71.
- (17) Sahoo, H. Förster resonance energy transfer—A spectroscopic nanoruler: Principle and applications. *J. Photochem. Photobiol., C* **2011**, *12*, 20–30.
- (18) Caldino, U.; Munoz, A.; Rubio, J. Energy transfer in CaCl₂: Eu: Mn crystals. *J. Phys.: Condens. Matter* **1993**, *5*, 2195.
- (19) Barry, T. L. Luminescent Properties of Eu²⁺ and Eu²⁺ Mn²⁺ Activated BaMg₂Si₂O₇. *J. Electrochem. Soc.* **1970**, *117*, 381–385.
- (20) Yao, G.; Lin, J.; Zhang, L.; Lu, G.; Gong, M.; Su, M. Luminescent properties of BaMg₂Si₂O₇: Eu²⁺, Mn²⁺. *J. Mater. Chem.* **1998**, *8*, 585–588.
- (21) Yang, W.-J.; Luo, L.; Chen, T.-M.; Wang, N.-S. Luminescence and energy transfer of Eu- and Mn-coactivated CaAl₂Si₂O₈ as a potential phosphor for white-light UVLED. *Chem. Mater.* **2005**, *17*, 3883–3888.
- (22) Huang, A.; Yang, Z.; Yu, C.; Chai, Z.; Qiu, J.; Song, Z. Tunable and white light emission of a single-phased Ba₂Y(BO₃)₂Cl: Bi³⁺, Eu³⁺ phosphor by energy transfer for ultraviolet converted white LEDs. *J. Phys. Chem. A* **2017**, *121*, 5267–5276.
- (23) Li, K.; Lian, H.; Han, Y.; Shang, M.; Van Deun, R.; Lin, J. BaLu₆(Si₂O₇)₂(Si₃O₁₀): Ce³⁺, Tb³⁺: a novel blue-green emission phosphor via energy transfer for UV LEDs. *Dyes Pigm.* **2017**, *139*, 701–707.
- (24) Zhang, S.; Li, Y.; Lv, Y.; Fan, L.; Hu, Y.; He, M. A full-color emitting phosphor Ca₉Ce(PO₄)₇: Mn²⁺, Tb³⁺: efficient energy transfer, stable thermal stability and high quantum efficiency. *Chem. Eng. J.* **2017**, *322*, 314–327.
- (25) Zhang, X.; Huang, Y.; Gong, M. Dual-emitting Ce³⁺, Tb³⁺ co-doped LaOBr phosphor: luminescence, energy transfer and ratiometric temperature sensing. *Chem. Eng. J.* **2017**, *307*, 291–299.
- (26) Liu, Z.; Li, Y.; Xiong, Y.; Wang, D.; Yin, Q. Electroluminescence of SrAl₂O₄: Eu²⁺ phosphor. *Microelectron. J.* **2004**, *35*, 375–377.